

Two Resistance Mass Transport Model for the Adsorption of Acid Dye onto Chitin in Fixed Beds

G. McKAY,* H. S. BLAIR, and J. R. GARDNER, *Department of Chemical Engineering, Queens University, Belfast, Northern Ireland*

Synopsis

A mass transport model has been developed to predict theoretical breakthrough curves in fixed bed adsorbers. The model has been tested using experimental data obtained for the adsorption of Acid Blue 25 on chitin. The effective diffusivity can be determined for the adsorption process by best fitting experimental and theoretical breakthrough curves and was found to be $5.5 \times 10^{-6} \text{ cm}^2 \text{ s}^{-1}$.

INTRODUCTION

Most industrial adsorption processes employ fixed bed adsorbers to remove pollutants from effluents. The ability of chitin to adsorb various dyestuffs has been reviewed and discussed previously by McKay et al.^{1,2} with particular reference to batch adsorption.

In terms of fixed bed adsorption one of the more successful simple modelling methods is the bed depth service time (BDST) model of Hutchins.³ This model assumed a linear relationship between the bed depth and the service time required for a chosen percentage content of impurity to reach the selected breakpoint in the bed. This model was applied to several fixed bed studies for the adsorption of various dyestuffs onto chitin by McKay et al.⁴ with considerable success. However, the model does not consider the mass transport kinetics of the adsorption process and therefore is limited in accuracy to the data under investigation and great care must be adopted in extending this model to predict design data.

Consequently, a model has been developed and presented in this paper. The model is based on external mass transport and pore diffusion, which is controlled by an effective diffusion coefficient. The actual rate and mechanism of the adsorption process, the nature of the isotherm, the flow rate, the effluent concentration, and the height of the bed, all contribute to the shape of the curve. This paper applies the mass transport model to the adsorption of Acid Blue 25 dye onto chitin and the effects of bed height and solution flow rate have been studied.

THEORY

Spahn and Schlunder⁵ used a method which assumed an irreversible isotherm, i.e., the solute concentration in the solid is independent of the

*To whom correspondence should be addressed.

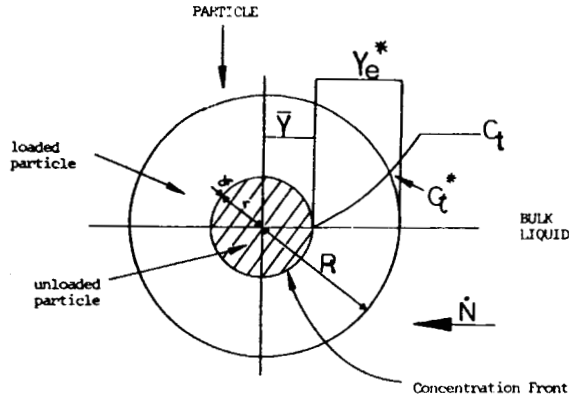


Fig. 1. Schematic representation of unreacted particle adsorption model.

concentration in the liquid phase. They dismissed a fairly simple analytical technique for establishing k_f and k_p (surface and internal mass transfer coefficients, respectively) based on homogeneous diffusion and predicted an "unreacted core" model of adsorption in the particle pores. The model is represented schematically in Figure 1. With the assumption of an irreversible equilibrium, the equilibrium concentration Y_e can be replaced by a hypothetical equilibrium concentration $Y_e^* = \text{const}$. This corresponds to the monolayer coverage indicated by the limiting condition of the favorable isotherm (i.e. separation factor $a \rightarrow 0$, irreversible equilibrium) represented in Figure 2. Because of the surface mass transfer resistance, C_t in the bulk liquid drops to C_t^* at the particle surface. The solute concentration in the pore liquid then drops from C_t^* at the surface to zero at internal radius r (concentration front). The mathematical analysis of this model is then developed for a single particle. The rate of adsorption N , is related to the surface mass transfer coefficient k_f by

$$\dot{N} = 4\pi R^2 k_f (C_t - C_t^*) \tag{1}$$

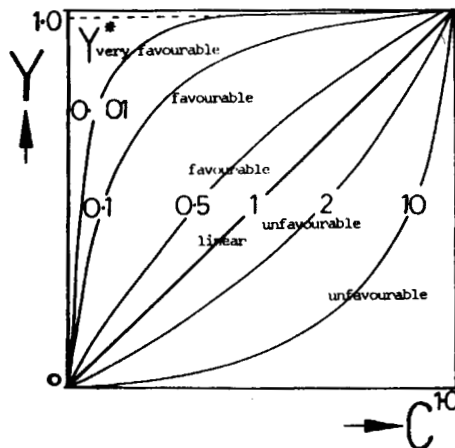


Fig. 2. Isotherm shapes for various separation factor, a , values.

\dot{N} is related to the effective diffusion coefficient D_e in the pore liquid by Fick's first law:

$$\dot{N} = \frac{4\pi D_e}{(1/r - 1/R)} C_t^* \tag{2}$$

where r is the radial distance the concentration front has reached within the particle. The velocity of the concentration front at $R = r$ is obtained from the mass balance for a spherical particle:

$$\dot{N} = -4\pi r^2 Y_e^* \rho \frac{dr}{dt} \tag{3}$$

The average concentration in the carbon \bar{Y} is given by

$$\bar{Y} = Y_e^* [1 - (r/R)^3] \tag{4}$$

Dimensionless parameters are then introduced:

$$\tau = \frac{C_0}{\rho Y_e^*} \frac{D_e t}{R^2} \tag{5}$$

$$\frac{\bar{Y}}{Y_e^*} = \eta \text{ and } \frac{C_t}{C_0} = \xi \tag{6}$$

and

$$\frac{k_f R}{D_e} = \text{Bi} \tag{7}$$

Using eqs. (5)–(7) and eqs. (1)–(4) the adsorption rate is given by

$$\frac{d\eta}{d\tau} = \xi \frac{3(1 - \eta)^{1/3}}{1 - [1 - (1/\text{Bi})](1 - \eta)^{1/3}} \tag{8}$$

The adsorption rate is therefore shown to be a function of the solute concentrations in the liquid phase, ξ , the solid phase, η , and of the Biot number Bi.

The rate equation for a single particle is now considered as a function of the dye concentration in the aqueous phase, ξ in the chitin phase, η , and the Biot number. The general form of the kinetic equation is shown:

$$\frac{\delta \eta}{\delta \tau} = \xi f(\eta)_{\text{Bi}} \tag{9}$$

The differential mass balance for the fixed bed column is given by

$$\frac{\delta \xi}{\delta \Psi} + \frac{\delta \eta}{\delta \tau} = 0 \tag{10}$$

Combining eqs. (9) and (10) yields a differential equation for the prediction of the local and time-dependent concentration history in the solid phase:

$$\frac{\delta^2 \eta}{\delta \tau \delta \Psi} \cdot \frac{f'(\eta)}{f(\eta)} \cdot \frac{\delta \eta}{\delta \tau} \cdot \frac{\delta \eta}{\delta \Psi} + \frac{\delta \eta f(\eta)}{\delta \tau} = 0 \quad (11)$$

The following general solution has been developed from the previous equations by Van Meel,⁶ Brauch and Schlunder,⁷ and McKay.⁸

$$\int_{\eta} \frac{\delta \eta}{\eta f(\eta)} = - \int_{\Psi} \delta \Psi \quad (12)$$

In order to evaluate eq. (12), it is necessary to divide the whole integration period into two periods. The first section represents that part of the adsorption bed it is necessary to saturate until a stable breakthrough is established. For the first section, the solution is of the form

$$\xi(\xi, \tau) = \frac{\eta(\Psi, \tau)}{\eta(0, \tau)} \quad (13)$$

For the second section

$$\xi(\Psi, \tau) = \eta(\Psi, \tau) \quad (14)$$

The model considered by the two previous equations was developed into a Fortran program and this was used to generate theoretical breakthrough curves. These curves have been compared with experimental data.

DISCUSSION

The results for the adsorption of Acid Blue 25 on chitin were chosen to test the model. The equilibrium isotherm for the dye is shown in Figure 3 and is of the Langmuir type with the monolayer beginning at approximately a concentration of 80 mg dm⁻³. The analysis of the data obeys the following equation:

$$Y_e = \frac{22.7C_e}{1 + 0.12C_e} \quad (15)$$

The mathematical development of the column model is fully described in the theory section. Using this column pore diffusion model, it was possible to predict the breakthrough curves for the AB 25-chitin system accurately with the aid of the computer program. The results in Figures 4-6 show theoretical lines compared with experimental points at three velocities for the adsorption of AB 25 on chitin at six bed heights. At higher flow rates the correlation

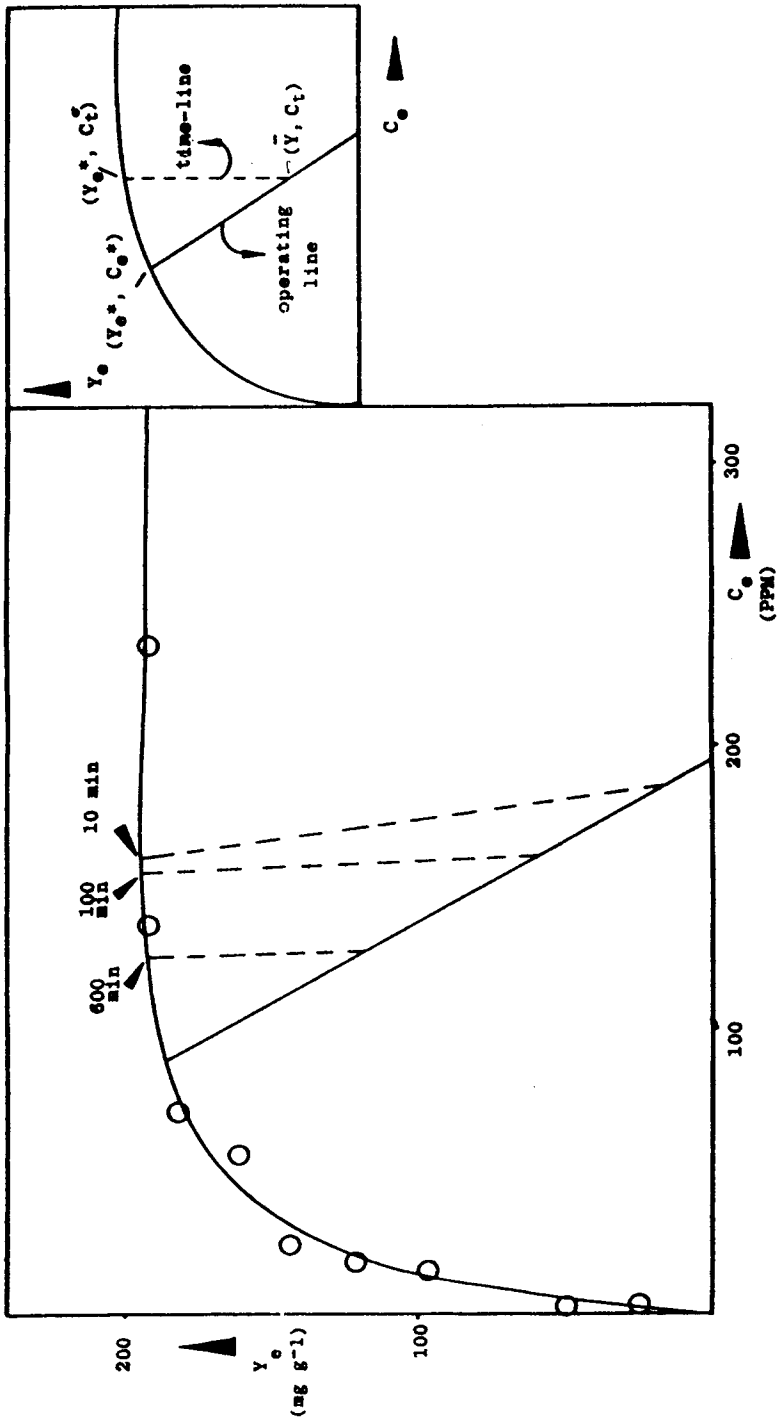


Fig. 3. AB 25 control isotherm showing operating and time-lines.

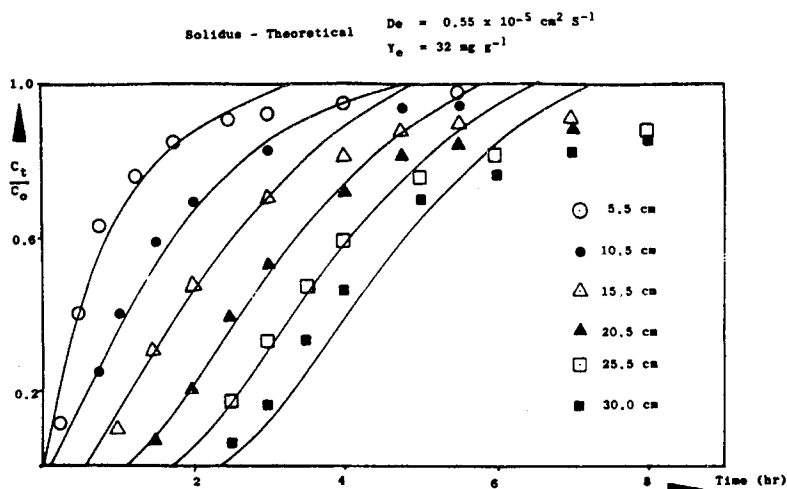


Fig. 4. Comparison of experimental and theoretical breakthrough curves—AB 25 at $120 \text{ cm}^3 \text{ min}^{-1}$.

between experimental and theoretical data was excellent but not as good at the lower dye solution flow rate. Graphical differentiation of the breakthrough curves gave equilibrium solid phase concentrations of 32 mg g^{-1} at flow rates of 82 cm^3 and $120 \text{ cm}^3 \text{ min}^{-1}$ but 36 mg g^{-1} at $38 \text{ cm}^3 \text{ min}^{-1}$. This apparent change in equilibrium capacity with velocity of dye solution may require a change in the effective diffusivity of the system to obtain a better fit at lower velocities. This phenomenon is further supported by the fact that an effective diffusivity of $0.55 \times 10^{-5} \text{ cm}^2 \text{ s}^{-1}$ was required to fit the column data in comparison to the $D_e = 0.50 \times 10^{-6} \text{ cm}^2 \text{ s}^{-1}$ used for the batch studies by McKay et al.⁹ All of the theoretical curves were obtained at a significantly higher equilibrium saturation capacity of 225 mg g^{-1} in the batch studies and therefore a substantial change in D_e is not unrealistic.

A typical set of the data fed into the column program along with some of the predicted data obtained from it are shown in Table I. The major deviation between experimental and theoretical data in the three figures (4–6) occurs at high adsorbent/high solution concentrations and is due to breakdown in the model assumptions. Under such conditions the assumption of irreversibility is no longer fully justified, and the theoretical breakthrough curves continue to rise steeply to the breakthrough values $C_t/C_0 \rightarrow 1.0$, whereas the experimental values begin to asymptote due to the limited amount of adsorption/desorption. Nevertheless, for the 18 curves shown in the diagrams, there is good agreement between the theoretical pore model data and the experimental results.

CONCLUSION

The adsorption of Acid Blue 25 onto chitin in fixed bed columns has been studied. The model, based on external mass transport and pore diffusion, was used to predict and compare theoretical breakthrough curves with experimental results. Using a best fit technique a pore diffusivity of $5.5 \times 10^{-6} \text{ cm}^2 \text{ s}^{-1}$ was found to apply to the system.

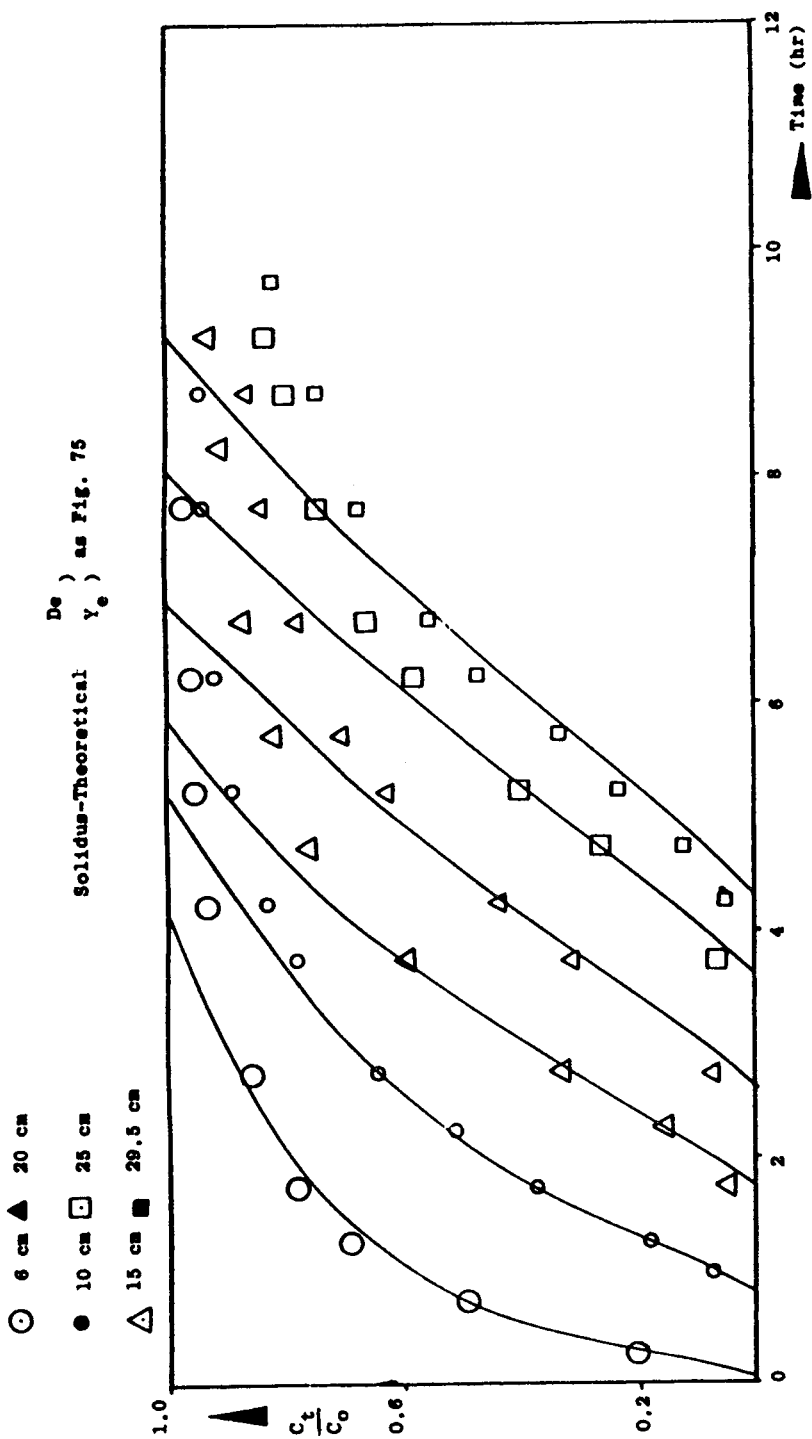


Fig. 5. Comparison of experimental and theoretical breakthrough curves—AB 25 at 82 cm³ min⁻¹.

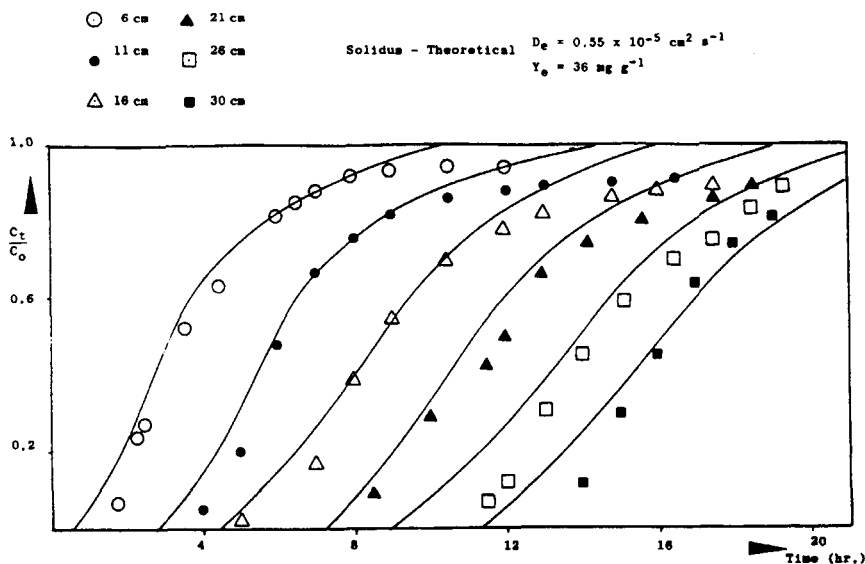


Fig. 6. Comparison of the experimental and theoretical breakthrough curves—AB 25 at $38 \text{ cm}^3 \text{ min}^{-1}$.

APPENDIX: NOMENCLATURE

- a dimensionless constant separation factor
 Bi Biot number
 C liquid phase solute concentration ($\text{ppm} = \text{mg dm}^{-3}$)
 C_e equilibrium liquid phase solute concentration
 C_0 initial liquid phase solute concentration
 C_e^* hypothetical equilibrium liquid phase solute concentration in the pores
 C_t liquid phase solute concentration at time t
 D_e effective pore diffusivity ($\text{cm}^2 \text{ s}^{-1}$)
 F flow rate in column studies ($\text{cm}^3 \text{ min}^{-1}$)
 k_f surface mass transfer coefficient (cm s^{-1})
 k_p internal mass transfer coefficient (cm s^{-1})
 N adsorption rate (mg s^{-1})
 r internal radial distance (cm)
 R full particle radius (cm)
 t time (s, min, h)
 Y solid phase solute concentration (mg g^{-1})
 \bar{Y} mean solid phase solute concentration in equilibrium with C_t
 Y_e equilibrium solid phase solute concentration
 Y_t solid phase solute concentration at time t

Greek Symbols

- ρ particle density (g cm^{-3})
 Ψ dimensionless capacity factor
 ξ dimensionless liquid phase solute concentration
 η dimensionless solid phase solute concentration
 τ dimensionless time

TABLE I
Column Data in Program Input^a

Effective diffusivity	DEFF =	0.550E - 05	CM2, SEC - 1
Particle density	DENS =	0.450E 00	G, CM - 3
Molecular diffusivity	DMOL =	0.500E - 05	CM2, SEC - 1
Effective particle diameter	DP =	0.855E - 01	CM
Flow rate	F =	0.136E 01	CM3, SEC - 1
Quantity of adsorbent	S =	0.100E 03	G
Service time of bed	T =	0.378E 05	SEC
Bed voidage fraction	VOID =	0.600E 00	(-)
Kinematic viscosity	VK =	0.100E - 01	CM2, SEC - 1
Initial dye con. in liquid	XO =	0.100E 00	MG.CM - 3
Equilibrium solid phase con.	YE =	0.320E 02	MG.G - 1
Length of adsorbent bed	Z =	0.295E 02	CM
Predicted Data			
Particle Reynolds number	RE =	0.122E 01	
Liquid mass transfer coefficient	BL =	0.933E - 03	CM.SEC - 1
Biot number	BI =	0.725E 01	
Dimensionless time when the first carbon later at the adsorber entrance is saturated	DTI =	0.213E 00	
Dimensionless service time	DTMX =	0.790E 00	
Dimensionless time interval	TNT =	0.790E - 02	

^aE = powers of 10; e.g., E - 05 = 10⁻⁵.

References

1. G. McKay, H. S. Blair, and J. R. Gardner, *J. Appl. Polym. Sci.*, **27**, 4251 (1982).
2. G. McKay, H. S. Blair, and J. R. Gardner *J. Appl. Polym. Sci.*, **28**, 1769 (1983).
3. R. A. Hutchins, *Chem. Eng.* **80**, 133 (1973).
4. G. McKay, H. S. Blair, and J. R. Gardner, *J. Appl. Polym. Sci.*, **29**, 1499 (1984).
5. H. Spahn and E. U. Schlunder, *Chem. Eng. Sci.* **30**, 529 (1975).
6. D. A. Van Meel, *Chem. Eng. Sci.*, **9**, 63 (1958).
7. V. Branch and E. U. Schlunder, *Chem. Eng. Sci.*, **30**, 539 (1975).
8. G. McKay, *Chem. Eng. Res. Des.*, **62**, 235 (1984).
9. G. McKay, *J. Appl. Polym. Sci.* **30**, 4325 (1985).

Received January 22, 1986

Accepted May 22, 1986